Extended Abstract:

Advancing Clay Management in Base Metal Flotation with Novel Chemistry

Oznur Onel[1] & Michelle Hoang[1]

[1] Nalco Water an Ecolab Company, Naperville, Illinois, USA

Clay minerals create significant challenges in flotation by affecting slurry rheology, froth stability, and surface interactions. Swelling types like montmorillonite increase viscosity through structured networks, while non-swelling clays such as kaolinite and muscovite primarily contribute to entrainment, surface sliming, and froth destabilization. This study investigates a novel chemistry designed to minimize the impact of clay-related issues, with particular focus on non-swelling varieties. Fundamental tests were conducted using synthetic chalcopyrite–clay systems, supported by flotation trials on samples from diverse ore bodies to validate field relevance. Zeta potential and rheological measurements revealed substantial improvements in slurry behavior for kaolinite - muscovite and montmorillonite-rich systems. Flotation performance consistently improved in terms of both recovery and selectivity. These results support a targeted and adaptable reagent strategy that addresses clay complexity in flotation circuits and contributes meaningfully to processing efficiency in high-clay ore environments.

Keywords: Clay minerals, flotation, dispersants, rheology, surface chemistry, base metals

1 Introduction

The global base metal industry faces an increasingly complex challenge as ore grades decline and mineralogical complexity intensifies. Among the most persistent obstacles to efficient flotation performance is the presence of clay minerals—phyllosilicates that fundamentally alter pulp rheology, surface chemistry, and separation efficiency. Clay minerals—phyllosilicate minerals with layered crystal structures—are ubiquitous gangue components in copper, nickel, lead, zinc, and molybdenum ores, particularly in weathered, supergene-enriched, and lateritic deposits. The presence of even modest quantities of clay (3-10 wt%) can dramatically impair flotation performance through mechanisms that extend far beyond simple dilution effects [1][8]. As operations worldwide transition to processing lower-grade, clay-bearing ores, the economic and technical imperative to develop robust clay management strategies has never been more critical.

Clay minerals fundamentally disrupt the physicochemical conditions required for selective froth flotation. They increase pulp viscosity by orders of magnitude, coat valuable mineral surfaces with hydrophilic layers, consume reagents non-selectively, alter water chemistry, stabilize froths that promote gangue entrainment, and create non-Newtonian flow behavior that impedes particle-bubble collision and attachment [3][15][6]. The economic consequences are substantial: reduced throughput, lower recovery and grade, increased reagent consumption, higher energy costs, and compromised downstream dewatering and tailings management [4][16].

Clay minerals represent a diverse family of layered aluminosilicates, each exhibiting unique physicochemical properties that dictate their specific interference mechanisms in flotation circuits. Understanding the nuanced behavior of different clay types—from the highly swelling montmorillonites to the edge-charged kaolinites and the naturally hydrophobic talcs—is essential for designing targeted mitigation strategies that preserve valuable mineral recovery while maintaining concentrate grade specifications.

The deleterious effects of clay minerals in base metal flotation manifest through well-characterized but complex mechanisms. Slime coating, perhaps the most widely recognized phenomenon, occurs when ultrafine clay particles adsorb onto valuable mineral surfaces, creating a hydrophilic barrier that prevents collector adsorption and reduces bubble-particle attachment probability. This mechanism is particularly pronounced with montmorillonite and kaolinite, where surface area considerations and edge-face charge heterogeneity drive strong electrostatic and van der Waals interactions with sulfide minerals [1][2].

Beyond surface coating, clay minerals dramatically alter pulp rheology, transforming Newtonian slurries into non-Newtonian, yield-stress fluids. Montmorillonite, with its exceptional swelling capacity and ability to form "house-of-cards" gel networks, can increase apparent viscosity by orders of magnitude even at modest concentrations (3-5 wt%) [3]. This rheological transformation impedes particle-bubble collision efficiency, reduces turbulent mixing, and constrains the operational flexibility of flotation circuits. The yield stress induced by clay networks requires higher energy input for particle suspension and creates dead zones within flotation cells where separation efficiency is compromised.

Reagent consumption represents another critical pathway of clay interference. The high specific surface area of clay minerals—ranging from 10-15 m^2/g for kaolinite to 600-800 m^2/g for montmorillonite—provides vast adsorption sites for collectors, frothers, and modifying reagents [4]. This non-selective adsorption not only increases operating costs but also disrupts the carefully balanced chemistry required for selective flotation. In saline water environments, increasingly common in water-stressed mining regions, the interaction between dissolved cations (Ca^{2+}, Mg^{2+}) and clay surfaces further complicates reagent performance through precipitation of hydroxide/carbonate species and compression of the electrical double layer [5].

The froth phase is equally vulnerable to clay-induced disruptions. Fine clay particles stabilize froth through increased liquid viscosity and film elasticity, promoting the mechanical entrainment of hydrophilic gangue and degrading concentrate grade. Simultaneously, clay minerals can alter bubble size distribution and coalescence behavior, affecting froth mobility and drainage characteristics. The net result is a trade-off between recovery and grade that often proves difficult to optimize without targeted chemical intervention [6].

Table 1. Comparative Summary: Clay Types and Flotation Impact

Clay Type	Structure	Swelling	CEC (meq/100g)	Surface Area (m^2/g)	Primary Flotation Impact
Montmorillonite	2:1 T-O-T	Strong osmotic & crystalline	80-150	600-800	Extreme viscosity, gel formation, slime coating, reagent consumption
Kaolinite	1:1 T-O	None	3-15	10-30	Slime coating (edge-face heterocoagulation), moderate entrainment
Illite	2:1 T-O-T (K^+ fixed)	Limited	10-40	65-100	Moderate slime coating, reagent consumption
Serpentine	1:1 Mg-rich	None(facet-dependent aggregation)	10-30	30-80	Heterocoagulation with sulfides, high viscosity, facet-selective coating
Talc	2:1 neutral	None	<5	3-10	Naturally floatable, increases froth viscosity, promotes entrainment
Chlorite	2:1:1	Minimal	10-40	50-150	Moderate slime coating, rheological effects

The mineral processing community has responded to the clay challenge with an evolving toolkit of chemical technologies, each designed to address specific aspects of clay interference. Traditional approaches centered on inorganic dispersants—sodium silicate, sodium hexametaphosphate, and polyphosphates—which function by adsorbing onto clay surfaces, increasing negative surface charge, and promoting electrostatic repulsion between particles. While effective at reducing viscosity and limiting slime coating, these reagents often lack selectivity and can inadvertently depress valuable minerals, particularly in alkaline circuits [7].

The limitations of conventional dispersants have driven innovation toward polymer-based solutions that offer enhanced selectivity and performance. Anionic polyacrylamides, carboxymethyl celluloses, and guar gum derivatives represent a class of high-molecular-weight polymers that sterically stabilize clay suspensions while minimizing interactions with sulfide minerals. Recent work has demonstrated that polymer architecture—molecular weight, charge density, and backbone rigidity—can be tuned to achieve clay-specific dispersion. For instance, studies show that certain anionic polymers preferentially adsorb onto the edge sites of kaolinite, neutralizing positive charges and preventing edge-face aggregation without significantly impacting chalcopyrite or pentlandite surfaces [8][9].

Selective flocculation represents a complementary strategy where high-molecular-weight flocculants are used to aggregate clay particles into settleable flocs that can be removed via desliming circuits prior to flotation. The ultra flocculation approach, employing optimized shear conditions (1000-1500 s^{-1}) and controlled flocculant dosing, has achieved >99.8% bentonite removal in laboratory studies, effectively decoupling clay management from the flotation circuit itself [10]. This physical removal strategy is particularly attractive for operations with extreme clay loadings where chemical dispersion alone proves insufficient.

The past five years have witnessed remarkable innovation in clay mitigation chemistry, driven by advances in nanotechnology, green chemistry, and process intensification. Nanoparticle-based collectors represent a paradigm shift in addressing slime coating. Polystyrene nanoparticles functionalized with cationic surfactants (e.g., St-CTAB) have demonstrated the ability to preferentially adsorb onto chalcopyrite surfaces in the presence of montmorillonite, creating a hydrophobic nanoparticle layer that resists clay coating and enhances collector (xanthate) adsorption. Bench-scale trials show that this dual-reagent approach can restore flotation kinetics to near-clay-free levels, with contact angle recovery from ~30° to >70° in montmorillonite-laden systems [1].

Chelating agents offer another innovative pathway, particularly for serpentine-bearing ultramafic ores. Sodium citrate, a benign organic chelator, has been shown to selectively complex with divalent cations (Mg^{2+}, Ca^{2+}) that mediate serpentine-pentlandite heterocoagulation. By removing these bridging cations, citrate reverses serpentine surface charge, disrupts slime coating, and restores pentlandite hydrophobicity. Field-relevant trials report nickel recovery increases from 74% to 96% with concomitant grade improvements from 11% to 15.1%, demonstrating the commercial viability of this green chemistry approach [11].

Electrochemical methods are emerging as energy-efficient alternatives for clay removal from process water streams. Electroflotation, utilizing saline water electrolysis to generate fine hydrogen bubbles at titanium cathodes, has achieved 91.4% removal of ultrafine kaolinite from recycled thickener overflow water. The synergy between electroflotation and in-situ electrocoagulation (from controlled anode dissolution) provides a dual mechanism for clay aggregation and removal, with implications for closed-water circuits in arid mining regions [12][13].

The integration of process intensification technologies—such as the Reflux Flotation Cell (RFC) with its downcomer and reverse fluidization bed—addresses clay entrainment through hydrodynamic control rather than chemical intervention alone. By maintaining low air fractions in the separation zone and providing a downward-flowing water curtain, the RFC physically rejects entrained clay particles while allowing hydrophobic minerals to report to the froth. Bench studies confirm superior grade-recovery performance compared to conventional mechanical cells in kaolinite-bearing systems [14].

The base metal industry stands at a critical juncture. Declining ore grades, increasing mineralogical complexity, and the imperative for sustainable, water-efficient operations demand that we advance beyond empirical clay management toward predictive, mechanism-based strategies. The research presented in this study spans the continuum from fundamental surface science—elucidating the molecular-scale interactions between clays, minerals, and reagents—to industrial-scale implementations that demonstrate economic benefits.

2 Materials and methods

2.1 Sample preparation

Porphyry copper ore samples were obtained from operating mines located in Latin America (LA) and North America (NA). All samples were stored in airtight containers and kept frozen to minimize oxidation and microbial alteration prior to flotation testing. The Latin America ore contained approximately 1.0 % Cu, while the North America ore contained about 0.5 % Cu. Both ores were crushed using a laboratory jaw crusher to achieve 100% passing 1 mm. The crushed material was then divided into 1.2 kg portions to serve as feed for laboratory rod milling. Grinding calibration was conducted using a 1.2 kg charge at a pulp density of 60 wt.% solids, targeting a P_{80} of 106 µm for the Latin America ore and 180 µm for the North America ore. The wet-ground products were used directly as flotation feeds. Chalcopyrite was identified as the major copper-bearing mineral in both samples. The dominant clay minerals were muscovite and kaolinite in the Latin America ore, and montmorillonite in the North America ore.

2.2 XRD Measurements

The Clay Speciation by XRD by XRD (ME-LR-MIN-MET-MN-D04) method used by SGS Natural Resources is accredited to the requirements of ISO/IEC 17025. Clay minerals are typically fine grained (<2µm) phyllosilicates in sedimentary rock. Due to the poor crystallinity and fine size of clay minerals, separation of the clay fraction from bulk samples by centrifuge is required. A slide of the oriented clay fraction is prepared and scanned followed by a series of procedures (the addition of ethylene glycol and high temperature heating). Clay minerals are identified by their individual diffraction patterns and changes in their diffraction pattern after different treatments.

2.3 Zeta Potential Measurement

Zeta potential measurements were performed to evaluate the electrokinetic behavior of chalcopyrite and representative clay minerals (kaolinite, montmorillonite, and illite) in the presence and absence of dispersants. Clay minerals were obtained from Sigma Aldrich, while chalcopyrite samples were sourced from VWR INTERNATIONAL LLC-USA. Measurements were conducted using an Anton Paar Litesizer 500 equipped with a dynamic light scattering (DLS) cell.

For each test, 0.1 g of mineral was suspended in 40 mL of deionized water and agitated for 5 minutes using a magnetic stirrer. The pH was adjusted to the desired level using 0.1 M HCl or 0.1 M NaOH. For alkaline conditions, lime ($Ca(OH)_2$) was used to adjust pH to 9 and 11, simulating plant practice. When dispersants were tested, they were introduced after pH stabilization and conditioned for an additional 3 minutes before sampling. A 3 mL aliquot was then drawn from the supernatant and transferred into the measurement cell. Each zeta potential value represents the average of three independent measurements under identical conditions.

2.4 Rheology Measurement

Rheological measurements were conducted using an Anton Paar MCR series rotational rheometer equipped with a serrated concentric cylinder (CC27) geometry to minimize wall slip. All tests were performed at 25 ± 0.1 °C under controlled shear rate mode. Synthetic pulps were prepared at 30 wt% solids by mixing 12 g of clay-bearing copper ore with deionized water. The sample contained approximately 16 wt% montmorillonite, representing a high-clay ore system. The slurry pH was adjusted to 8 using hydrated lime ($Ca(OH)_2$) to simulate plant conditions. Dispersant reagents were added at the desired dosages, and the pulp was conditioned for 2 min before testing. The slurry was then loaded into the rheometer cup, covered with a solvent trap, and allowed to equilibrate for 2 min prior to measurement. Flow curves were obtained over a shear-rate range of 0.1–100 s^{-1} to determine apparent viscosity and yield stress, followed by a three-interval thixotropy (3-ITT) test consisting of a high-shear interval (500 s^{-1}, 60 s), a low-shear recovery interval (1 s^{-1}, 600 s), and a final high-shear interval (500 s^{-1}, 60 s). The flow data were fitted to the Herschel–Bulkley model to determine yield stress and flow index, while thixotropic recovery (%) was calculated from the change in apparent viscosity during the recovery interval.

2.5 Flotation reagents

All flotation reagents, including collectors, frothers, and dispersants, were supplied by Nalco Water. The reagent suite and dosages used for each ore are summarized in Table 2. Potassium amyl xanthate (PAX) served as the primary collector, with auxiliary collector C411 used for the Latin America (LA) ore to improve chalcopyrite selectivity. Frothers F189-13 and FP607 were applied according to ore type to maintain froth stability. Two polymeric dispersants, FreeFlote 903 and FreeFlote 2244, were evaluated at varying dosages to assess their effect on pulp dispersion and flotation performance.

Table 2 Flotation reagents and dosages used in flotation experiments.

Reagents	Type	Dosage (g/t) LA	Dosage (g/t) NA
Collector	Potassium Amyl Xanthate PAX	17	50
	C411	25	-
Frother	F189-13	-	100
	FP607	6	-
Dispersant	FreeFlote 903	20-100-150	75-100-250-500
	FreeFlote 2244	20	100 -150

2.6 Flotation tests

Rougher flotation experiments were conducted separately for each ore type using 600 g of sample in a 1.2 L FLS laboratory flotation cell. The impeller speed was maintained at 650 rpm for the LA ore and 800 rpm for the NA ore, with pulp solids maintained at 30 wt.%. The pH was adjusted to 9.5 for the LA ore and 8.0 for the NA ore using lime ($Ca(OH)_2$).

Each test followed a standardized reagent addition sequence: 1 minute of dispersant conditioning, followed by 1 minute of collector addition, and 1 minute of frother conditioning prior to air introduction. Flotation was conducted for a total of 10 minutes for the LA ore and 20 minutes for the NA ore, with air flow rates of 5 L/min and 4 L/min, respectively. Concentrates were collected at 15-second intervals to generate grade–recovery profiles.

At the completion of each test, the concentrates and tailings were filtered, oven-dried, and weighed to calculate Cu recovery and grade. All experiments were performed in duplicate, and the average values with associated error bars are presented in the corresponding figures.

3 Results and discussion

3.1. XRD Tests Results

As shown in Table 3 and 4, the semi-quantitative X-ray diffraction analysis reveals distinct mineralogical characteristics for the two high-clay copper ores. The Latin America sample is primarily composed of quartz (41.9 wt%), muscovite (32.2 wt%), and chlorite (11.9 wt%), with minor contributions from pyrite and albite, indicating a silicate-dominated system rich in non-swelling phyllosilicates. In contrast, the North America sample contains substantial albite (30 wt%) and orthoclase (7.7 wt%), along with 16.2 wt% montmorillonite and smaller quantities of kaolinite and illite, suggesting the presence of swelling clays with higher water retention capacity. Both ores contain more than 10 wt% total clay minerals, but their differing clay compositions imply distinct processing challenges: the Latin America ore is expected to exhibit strong froth entrainment and surface sliming due to fine muscovite and chlorite particles, whereas the North America ore is more prone to rheological complications and pulp viscosity increases associated with montmorillonite. These differences highlight the need for tailored dispersant and reagent strategies for each ore type.

Table 3 Semi- quantitative X-Ray diffraction results

Mineral	Latin America Cu Ore (wt %)	North America Cu Ore (wt %)
Quartz	41.9	11
Muscovite	32.2	11
Albite	-	30
Pyrite	4.8	1.4
Chlorite	11.9	0.9
Orthoclase	-	7.7
Siderite	-	9.4
Ankerite	-	5.1
Chalcopyrite	3.9	1.2
Magnetite	-	-
Diopside	-	-
Calcite	1.0	1.0
Rutile	0.6	0.7
Hematite	-	-
	Clay	
Montmorillonite	0.6	16.2
Illite	1.6	1.2
Corrensite	-	3.9
Kaolinite	1.4	0.7
TOTAL	100	100

Table 4 Chemical compositions of minerals

Mineral	**Composition**
Quartz	SiO_2
Muscovite	$KAl_2(AlSi_3O_{10})(OH)_2$
Albite	$NaAlSi_3O_8$
Pyrite	FeS_2
Chlorite	$(Fe,Mg,Mn)_5Al(Si_3Al)O_{10}(OH)_8$
Orthoclase	$KAlSi_3O_8$
Siderite	$FeCO_3$
Ankerite	$CaFe(CO_3)_2$
Chalcopyrite	$CuFeS_2$
Magnetite	Fe_3O_4
Diopside	$CaMgSi_2O_6$
Calcite	$CaCO_3$
Bernalite	$Fe(OH)_3$
Rutile	TiO_2
Hematite	Fe_2O_3
Montmorillonite	$(Na,Ca)_{0.3}(Al,Mg)_2Si_2O_{10}(OH)_2\cdot nH_2O$
Illite	$(K,H_3O)(Al,Mg,Fe)_2(Si,Al)_4O_{10}[(OH)_2,(H_2O)]$
Kaolinite	$Al_2Si_2O_5(OH)_4$
Corrensite	$(Mg,Al)_9(Si,Al)_8O_{20}(OH)_{10}\cdot 4H_2O$

3.2 Zeta potential results

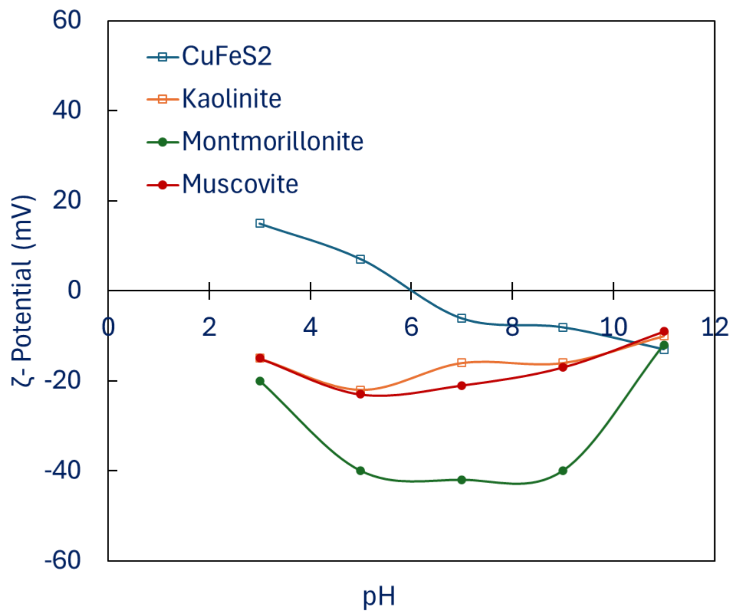

Figure 1. Zeta potential values at various pH for different clay types.

Figure 1 presents the variation of zeta potential as a function of pH for chalcopyrite ($CuFeS_2$) and three clay minerals—kaolinite, montmorillonite, and muscovite. The results indicate that all minerals exhibit negative surface charge across most of the tested pH range, with the magnitude increasing (i.e., becoming more negative) as pH rises. Chalcopyrite shows an isoelectric point near pH 5–6, transitioning from slightly positive to negative values above this pH, which is consistent with the hydrolysis of surface Cu^+/Fe^{2+} sites and the formation of $Cu(OH)_2$ and $Fe(OH)^+$ species. Among the clay minerals, montmorillonite displays the most negative potential (approximately −40 to −50 mV between pH 6–10), reflecting its high permanent charge arising from isomorphic substitution and its large cation exchange capacity. Kaolinite and muscovite show comparatively less negative zeta potentials (around −20 to −30 mV), consistent with their lower surface charge densities and pH-dependent edge sites. The overall trend confirms that swelling clays like montmorillonite create highly charged, electrostatically stable suspensions, whereas non-swelling clays (kaolinite, muscovite) and sulfide minerals (chalcopyrite) maintain more moderate surface charge behavior.

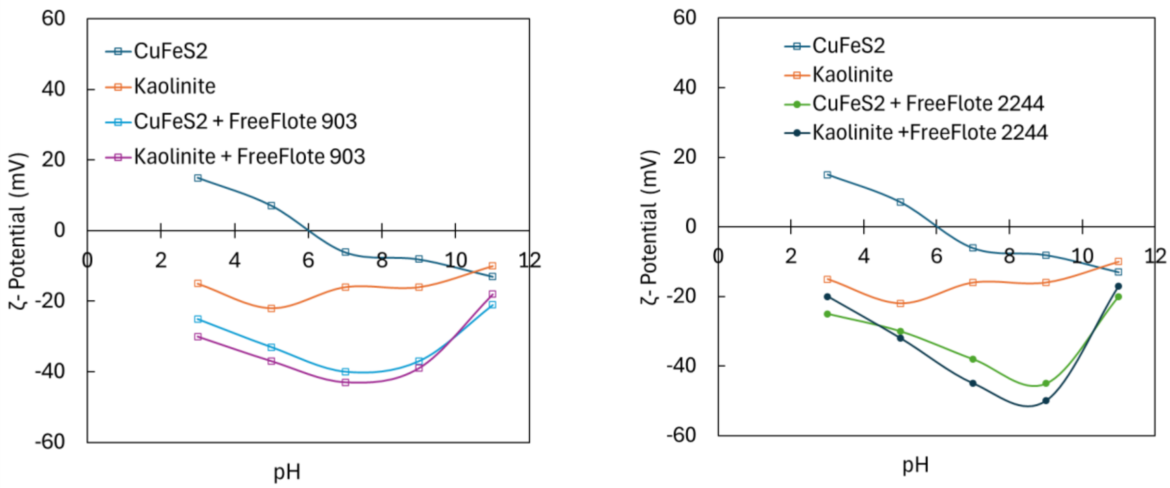

Figure 2. Effect of FreeFlote 903 and FreeFlote 2244 on the zeta potential of kaolinite - chalcopyrite systems.

The zeta potential results in Figure 2 reveal distinct electrokinetic responses of kaolinite–chalcopyrite systems to the two polymeric reagents. In both cases, the addition of dispersant shifted the overall potential toward more negative values across the pH range, indicating adsorption of anionic functional groups—carboxylate and sulfonate species—on the mineral surfaces. This shift suggests increased electrostatic repulsion between particles, promoting dispersion and mitigating slime coating.

For FreeFlote 903, the surface charge of both kaolinite and chalcopyrite became more negative by approximately 10–20 mV, with the most pronounced effect around pH 8–10, where the natural flotation of chalcopyrite is typically performed. This suggests that FreeFlote 903 effectively adsorbs on both mineral types, enhancing system stability and preventing hetero-aggregation between clay and sulfide particles.

In contrast, FreeFlote 2244 generated a stronger negative potential, particularly for kaolinite at pH values above 6, reaching nearly −50 mV around pH 9–10. This more substantial shift implies a higher degree of surface coverage or stronger adsorption affinity compared to FreeFlote 903, potentially due to its higher charge density or different molecular conformation in solution. However, excessively negative surface potentials could reduce particle–bubble attachment probability if overdosage occurs, suggesting that reagent dosage optimization is critical to maintain flotation selectivity.

Overall, both dispersants improved suspension stability, but FreeFlote 2244 exhibited a more pronounced electrokinetic impact, likely offering better control over kaolinite dispersion while requiring careful dosage management to avoid overdispersion and loss of hydrophobic mineral recovery.

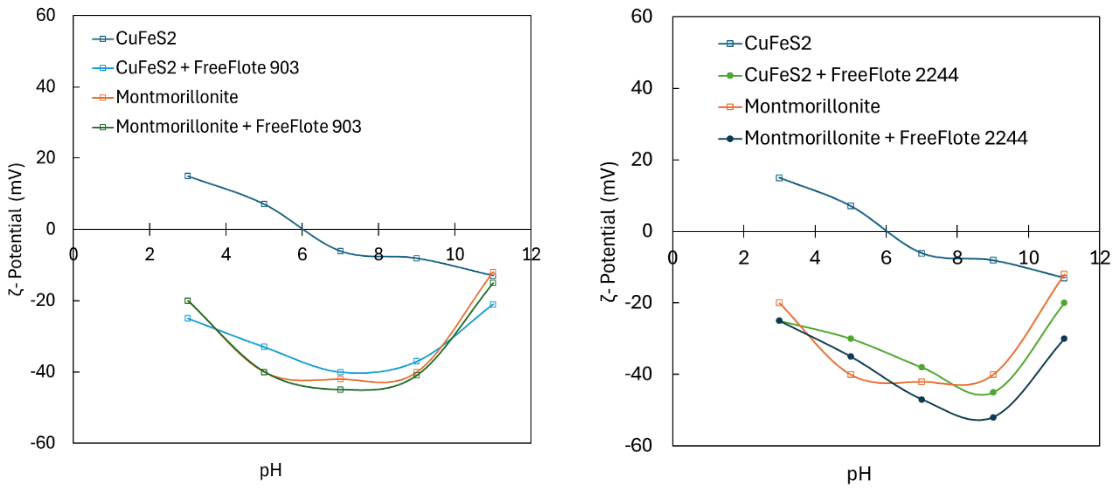

Figure 3. Effect of FreeFlote 903 and FreeFlote 2244 on zeta potential of montmorillonite – chalcopyrite systems.

The zeta potential measurements presented in Figure 3 demonstrate that both dispersants modify the electrokinetic behavior of montmorillonite–chalcopyrite suspensions, but with notably different magnitudes and trends compared to those observed for kaolinite systems. Montmorillonite inherently exhibits the most negative potential among the tested materials (approximately −40 to −50 mV across pH 6–10), due to its permanent structural charge arising from isomorphic substitution within the TOT layers. The addition of either FreeFlote 903 or FreeFlote 2244 resulted in only a minor additional shift toward negative values, suggesting limited adsorption of the dispersant molecules onto the already strongly charged montmorillonite surface. This observation indicates that the anionic functional groups of both reagents experience electrostatic repulsion from the negatively charged basal planes, leading to weak interaction and minimal alteration in the diffuse double layer.

For chalcopyrite, the dispersants induced a moderate negative shift in zeta potential—about 10–15 mV at pH 8–10—consistent with surface complexation between anionic polymer groups and positively charged metal hydroxide sites (Cu^{2+}/Fe^{2+} species). However, the overall electrokinetic response of the mixed system remained dominated by the montmorillonite component, reflecting the strong surface area and charge density effect of the clay. Between the two reagents, FreeFlote 2244 produced a slightly greater negative potential change, implying a higher degree of interaction with the montmorillonite edges or exchangeable interlayer cations compared to FreeFlote 903, though the effect was still modest relative to the non-swelling clays.

These findings suggest that dispersant performance is strongly clay-type dependent. For swelling clays such as montmorillonite, the reagent–surface interaction is constrained by permanent charge and high hydration forces, resulting in limited modification of surface potential. Consequently, the control of pulp rheology and particle dispersion in montmorillonitic systems may rely more on steric stabilization and viscosity regulation rather than electrostatic repulsion alone. This distinction underlines the importance of tailoring reagent chemistry not only to surface charge but also to the structural and hydration characteristics of the clay present in the ore.

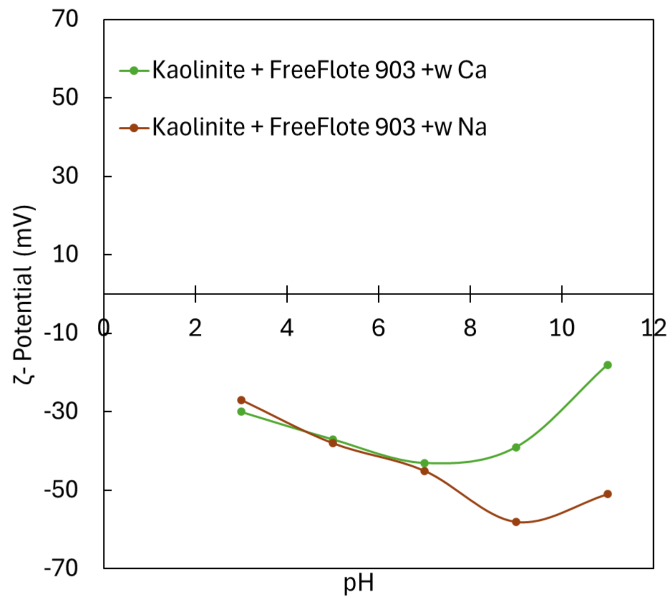

Figure 4. Effect of pH regulator $Ca(OH)_2$ and NaOH on the zeta potential of kaolinite in the presence of FreeFlote 903.

The results in Figure 4 show that the nature of the pH-modifying reagent significantly influences the electrokinetic behavior of kaolinite–dispersant systems at basic pH. When NaOH was used, the zeta potential became progressively more negative with increasing pH, reaching values around −50 mV near pH 10–11. This trend is attributed to the deprotonation of ≡Al–OH and ≡Si–OH surface groups and the limited interaction of monovalent Na^+ ions with the mineral surface, which primarily act as background electrolyte species. As a result, the system maintains a highly stable and dispersed suspension dominated by electrostatic repulsion.

In contrast, the use of $Ca(OH)_2$ resulted in a less negative potential and even a reversal toward positive values above pH 10. The presence of divalent Ca^{2+} ions promotes specific adsorption and surface complexation (≡Si–O–Ca^+, ≡Al–O–Ca^+) on negatively charged kaolinite sites, leading to double-layer compression and partial charge neutralization. Moreover, localized precipitation of $Ca(OH)_2$ or formation of Ca–clay bridges may induce partial flocculation, reducing suspension stability.

From an operational standpoint, the use of calcium-based reagents such as $Ca(OH)_2$ or $CaCO_3$ in flotation circuits is not only intended for pH control but also serves an important selective depression function, particularly for iron-bearing sulfides such as pyrite. Calcium species can adsorb on FeS_2 surfaces, forming $Fe(OH)_x$–Ca^{2+} complexes that hinder collector chemisorption and depress pyrite flotation. Therefore, the observed positive shift in zeta potential at high pH in the presence of Ca^{2+} reflects this broader role of calcium as both a pH regulator and a depressant.

3.3 Rheology measurement results

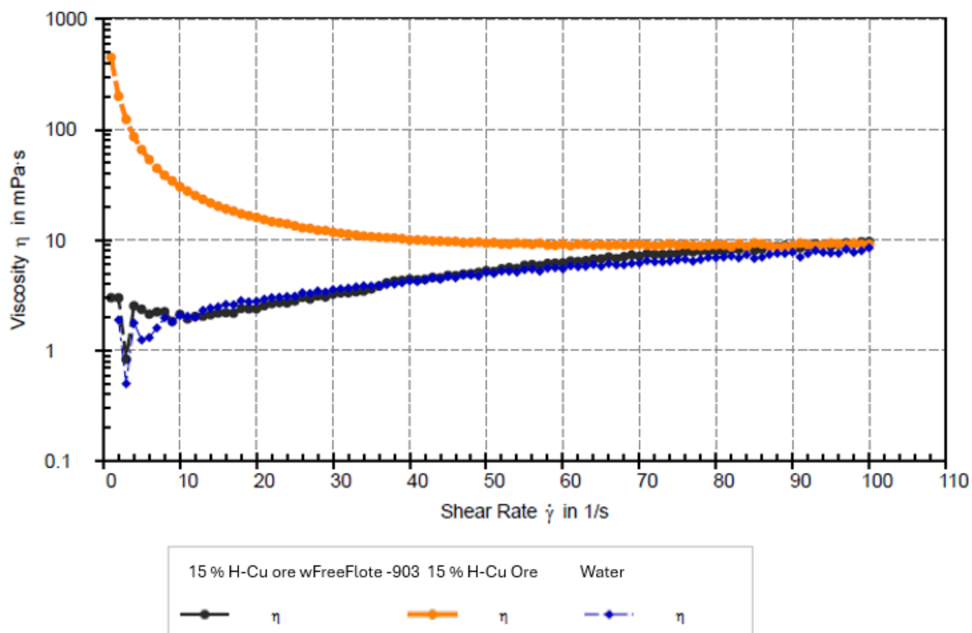

Figure 5. Apparent viscosity as a function of shear rate for 15% H–Cu ore and dispersant-treated samples (FreeFlote-903).

The untreated slurry (orange curve) in Figure 5 exhibited a pronounced shear-thinning behavior with extremely high viscosity at low shear rates, reaching nearly three orders of magnitude higher than water. This reflects the formation of a three-dimensional montmorillonite network, typical of swelling clay systems. Upon addition of FreeFlote-903, the viscosity markedly decreased across the entire shear-rate range, indicating disruption of the flocculated structure and enhanced particle dispersion. The similarity of the treated sample to water-like flow behavior confirms that the reagent effectively reduced interparticle associations and improved slurry fluidity.

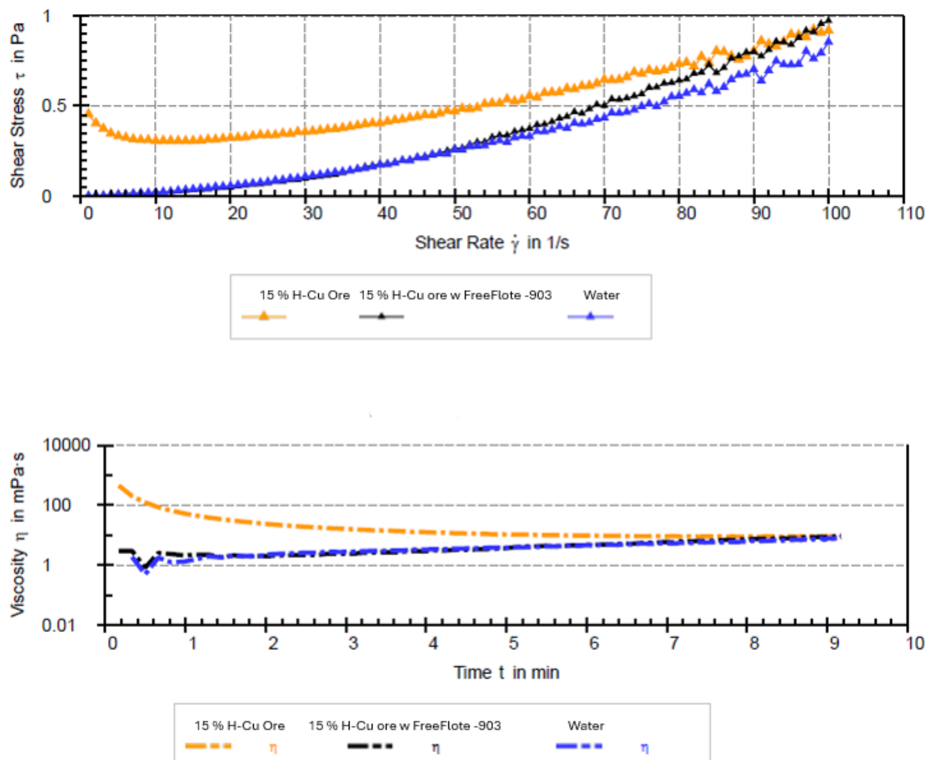

Figure 6. Shear stress–shear rate and time-dependent viscosity curves for 15% H–Cu ore and FreeFlote-903-treated pulp.

The shear stress–shear rate relationship shows a distinct yield stress for the untreated ore, which progressively declines with dispersant addition. As shown in Figure 6, the FreeFlote-903-treated pulp displays lower shear stress values at comparable shear rates, signifying a weakened structural network. The time-dependent viscosity curve further demonstrates that the untreated sample exhibits thixotropic decay followed by partial recovery, while the treated pulp maintains nearly constant viscosity. This behavior indicates that FreeFlote-903 effectively suppressed network rebuilding and stabilized the dispersion over time.

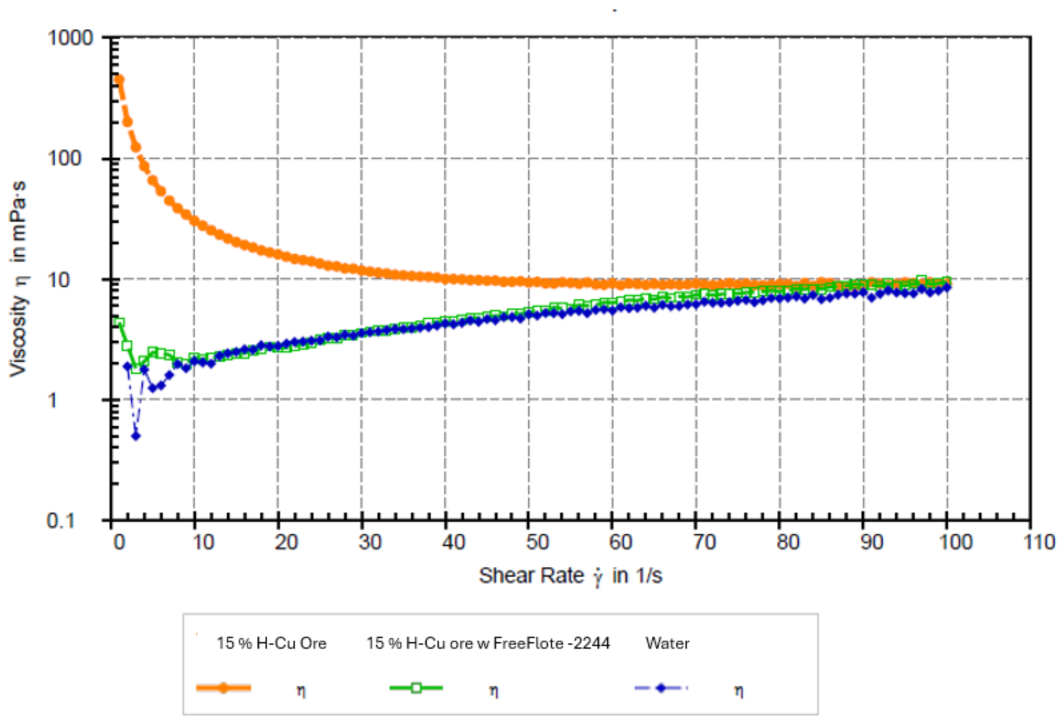

Figure 7. Apparent viscosity as a function of shear rate for 15% H–Cu ore and FreeFlote-2244-treated pulp.

Similar to FreeFlote-903, the addition of FreeFlote-2244 significantly reduced the apparent viscosity of the montmorillonite-rich slurry as shown in Figure 7. However, the viscosity reduction achieved with FreeFlote-2244 was slightly greater, especially at low shear rates, suggesting stronger dispersion and more efficient disruption of the montmorillonite gel structure. The nearly parallel trend between the treated pulp and the water baseline at high shear rates confirms that the pulp transitioned from a structured to a flowable state upon reagent addition.

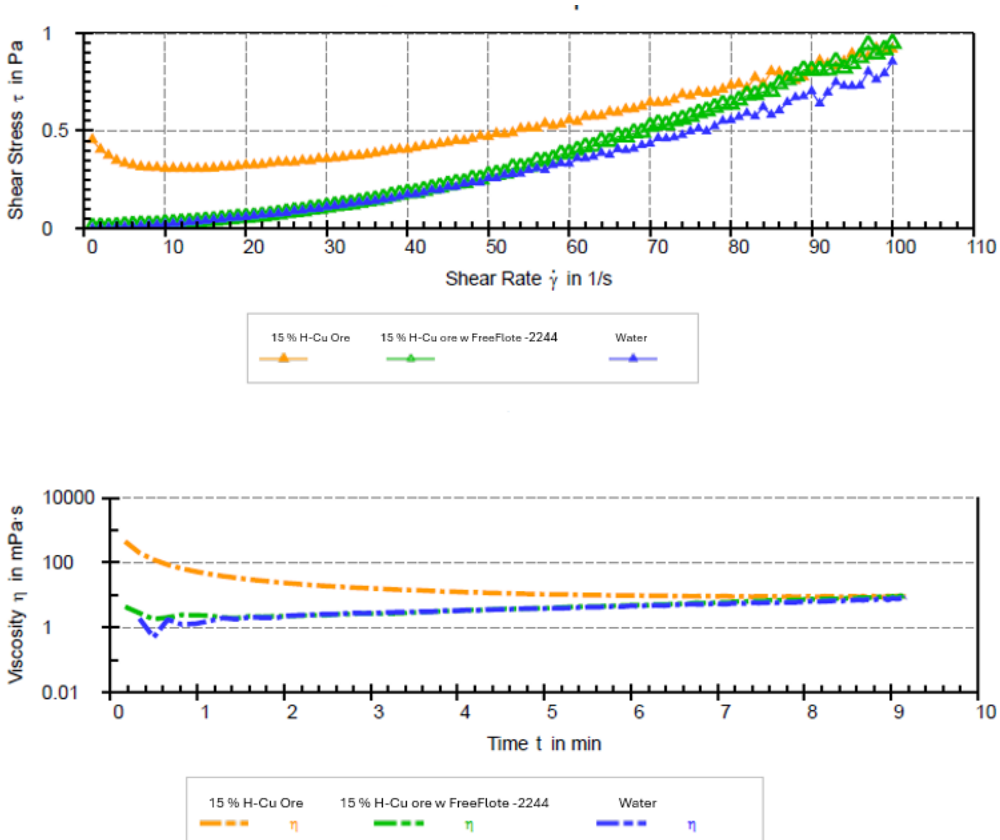

Figure 8. Shear stress–shear rate and time-dependent viscosity curves for 15% H–Cu ore and FreeFlote-2244-treated pulp.

In Figure 8, the untreated ore shows a non-linear τ–$\dot{\gamma}$ relationship with an apparent yield stress near 0.5 Pa, indicative of a cohesive clay network. In contrast, FreeFlote-2244-treated pulp exhibits substantially lower shear stress throughout the shear-rate range, consistent with a dispersed suspension. The time-dependent data reveal that while the untreated pulp undergoes viscosity relaxation over several minutes, the FreeFlote-2244-treated sample remains steady, confirming suppression of thixotropy and improved rheological stability.

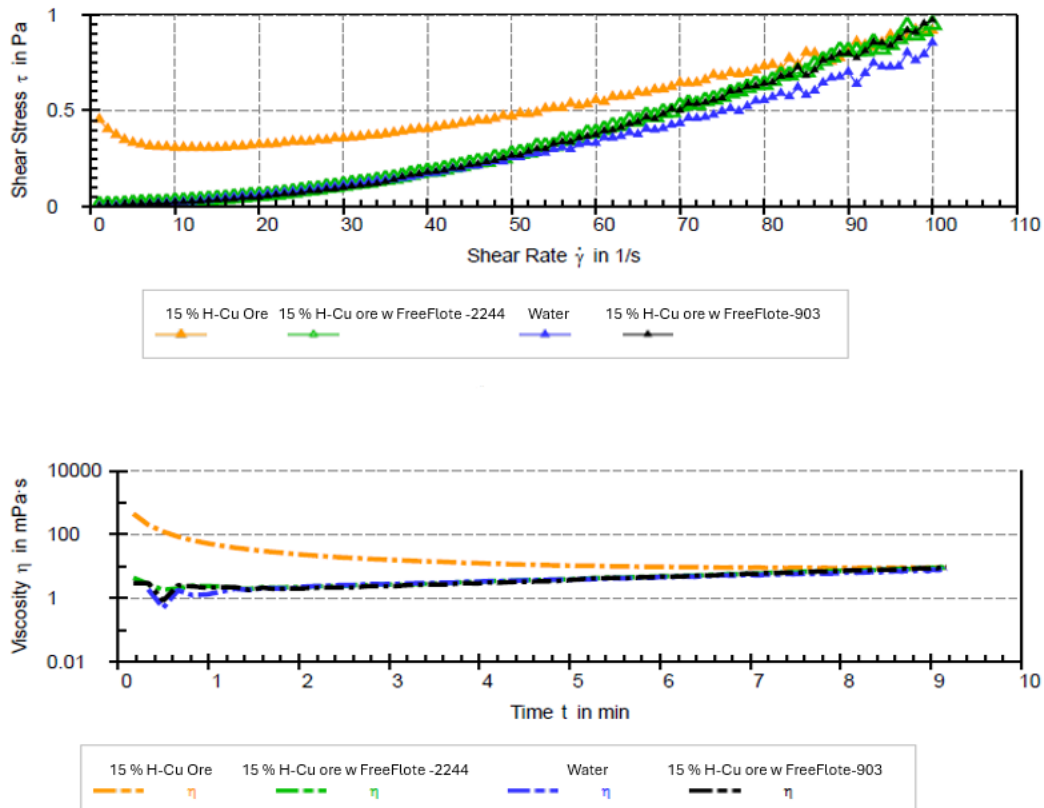

Figure 9. Comparative rheological behavior of 15% H–Cu ore with both dispersant chemistries (FreeFlote-2244 and FreeFlote-903).

Both dispersants effectively lowered the apparent viscosity and yield stress of the montmorillonite-containing pulp. Among them, FreeFlote-2244 exhibited slightly superior performance, yielding the lowest viscosity and most linear τ–$\dot{\gamma}$ profile. The convergence of both dispersant curves toward the water baseline indicates a high degree of stabilization and minimal network formation. These results demonstrate that while both reagents improve dispersion, the efficacy varies depending on the polymer chemistry and interaction with the clay surfaces.

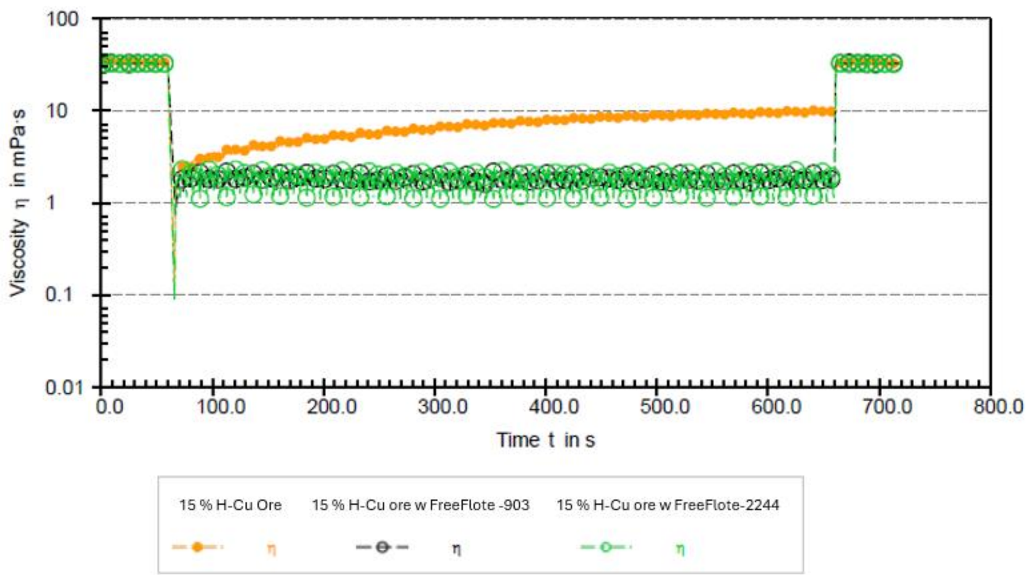

Figure 10. Three-interval thixotropy (3-ITT) test results for 15% H–Cu ore with and without dispersants.

As given in Figure 10, during the low-shear recovery interval, the untreated ore displayed gradual viscosity rebuilding, typical of thixotropic montmorillonite suspensions. In contrast, both dispersant-treated samples (FreeFlote-2244 and FreeFlote-903) exhibited significantly lower viscosity and nearly constant response, confirming that the flocculated network structure was effectively disrupted and could not rebuild over time. The results clearly demonstrate that dispersant addition provides slurry stabilization by suppressing structural reformation and maintaining a dispersed state, essential for improved flotation hydrodynamics.

3.4 Effect of Dispersants on flotation performance

3.4.1 Latin America Copper Ore Flotation Test Results

The results (in Figure 11) demonstrate a clear enhancement in flotation kinetics and selectivity with the addition of FreeFlote-903 (100 g/t) relative to the baseline. The FreeFlote-903 curve exhibits a consistently higher Cu grade at equivalent recovery levels and a faster approach toward the maximum cumulative recovery. The high coefficients of determination (R^2 = 0.9735–0.993) indicate excellent consistency and reproducibility of the experimental data. The steeper initial slope of the FreeFlote-903 recovery curve suggests an increased proportion of fast-floating particles and improved bubble–particle attachment efficiency. This improvement is attributed to more effective dispersion of non-swelling phyllosilicates such as muscovite and kaolinite, leading to cleaner chalcopyrite surfaces and enhanced selectivity under identical collector–frother conditions.

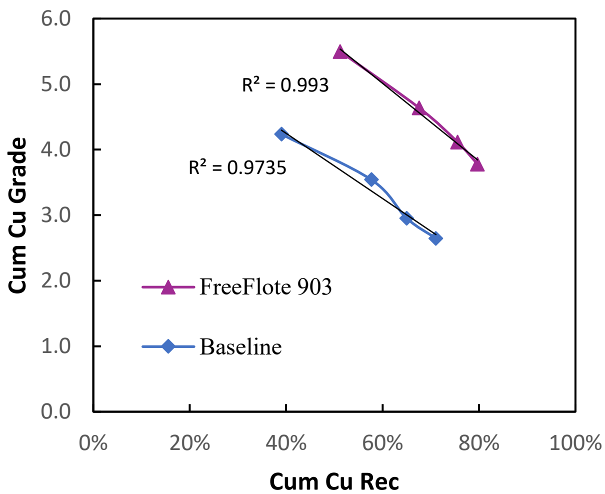

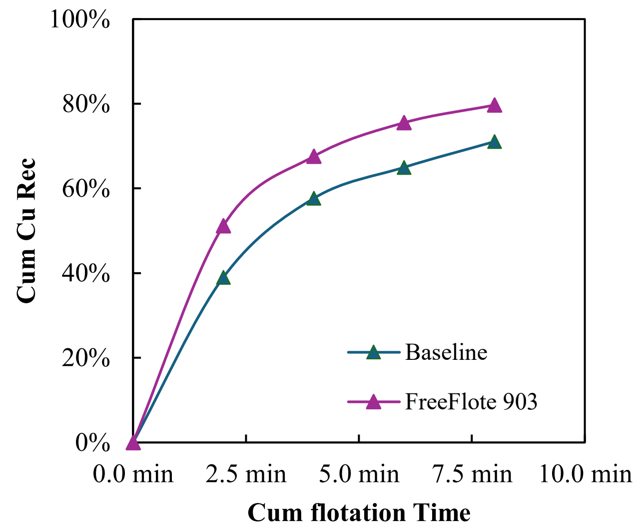

Figure 11. Flotation kinetics of the LA copper ore

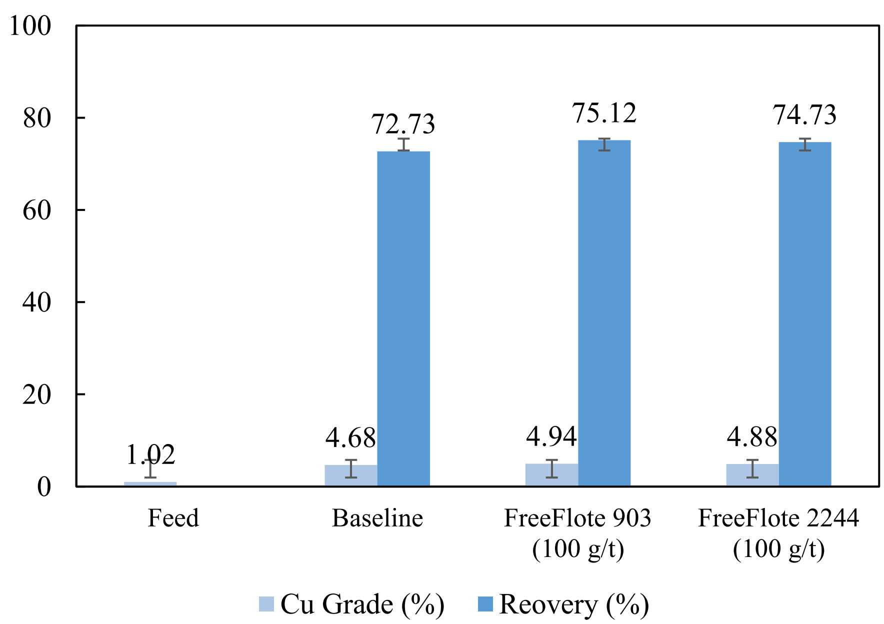

Figure 12. Effect of FreeFlote-2244 on LA Cu- Ore with 17 g/t PAX, 25 g/t C411 and 6 g/t FP607.

Figure 12. Effect of FreeFlote-903 and FreeFlote-2244 on the Latin America copper ore at fixed collector and frother conditions. Both reagents shift the grade–recovery curve upward relative to baseline, confirming efficient suppression of phyllosilicate sliming. FreeFlote-2244 at 20 g per t delivers the highest recovery at comparable grade, reaching 75.82 percent Cu recovery at 4.71 percent Cu grade, while FreeFlote-903 at 100 g per t attains 75.12 percent recovery at 4.94 percent grade. The superior displacement of the curve is fully consistent with the measured zeta potential

separation between chalcopyrite and clays and with the modest rheology change observed for this non-swelling clay system, indicating a surface-cleaning rather than bulk-flow mechanism.

The flotation results for the Latin America copper ore demonstrate a clear improvement in metallurgical performance with dispersant addition compared to the baseline. As shown in Figure 1, both FreeFlote-903 and FreeFlote-2244, applied at equal dosages of 100 g/t, enhanced copper recovery while maintaining comparable or slightly higher concentrate grades. FreeFlote-2244 achieved 75.12 percent recovery at 4.94 percent Cu grade, marginally outperforming FreeFlote-903, which yielded 74.73 percent recovery at 4.88 percent grade. This indicates that dispersant action primarily improved particle dispersion and reduced surface slime coating without adversely affecting selectivity.

The observed response is consistent with the ore's mineralogical composition, dominated by non-swelling phyllosilicates such as muscovite and chlorite, where the key limitation is surface contamination rather than rheological resistance. Electrokinetic measurements confirmed that both dispersants rendered clay particles more negatively charged, reducing their affinity for chalcopyrite surfaces. Consequently, the enhanced recovery arises from improved particle–bubble attachment efficiency rather than bulk slurry thinning. Overall, the results validate the use of moderate dispersant dosage as an effective strategy for mitigating clay-induced losses in non-swelling, silicate-rich copper ores.

3.4.2 North America Copper Ore Flotation Test Results

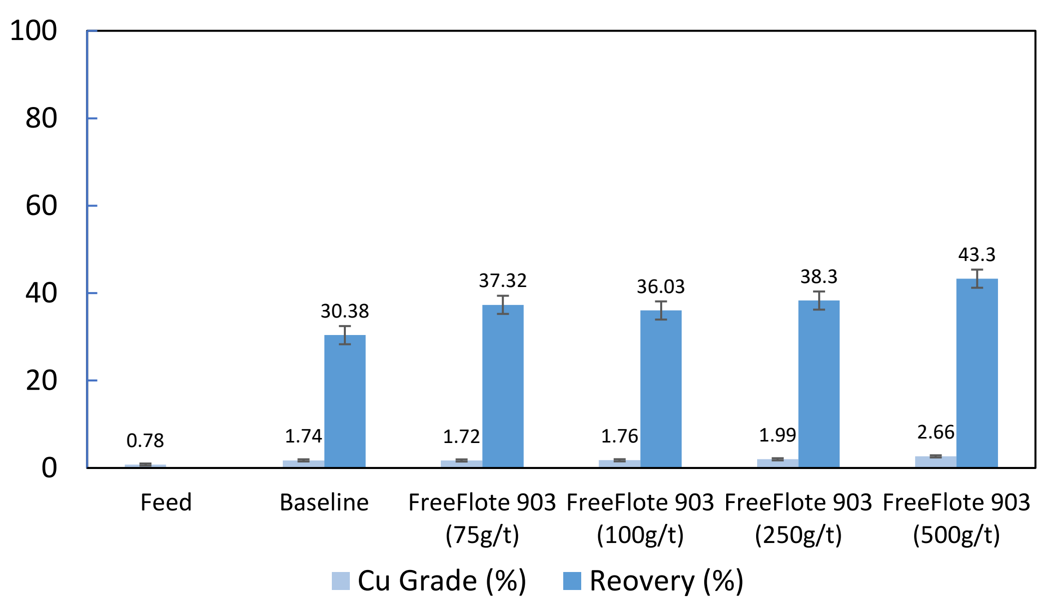

Figure 13. Effect of FreeFlote-903 dosage on the North America copper ore.

The grade–recovery trends in Figure 13 demonstrate a clear dispersant dosage dependence. At lower dosages (75–100 g/t), FreeFlote-903 modestly improves Cu recovery compared to the baseline, while higher additions (250–500 g/t) produce a pronounced upward shift in both recovery and grade, achieving 43.3 percent recovery at 2.66 percent Cu grade. This improvement aligns with the rheological observations where polymer addition significantly reduced slurry yield stress and improved particle dispersion, confirming that effective mitigation of swelling clay aggregation enhances bubble–particle attachment efficiency.

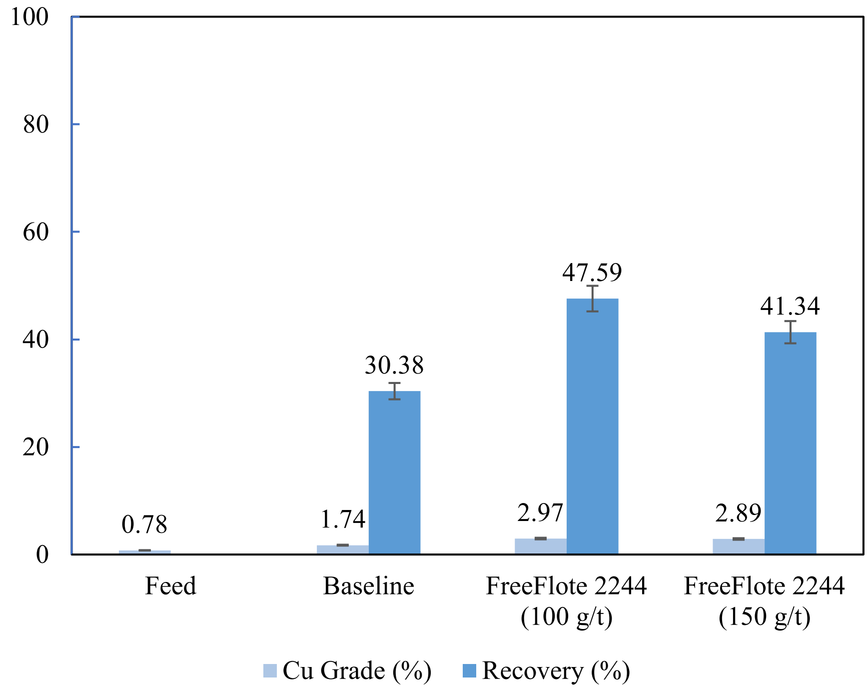

Figure 14. Effect of FreeFlote-2244 dosage on the North America copper ore.

Both 100 and 150 g/t dosages deliver substantial metallurgical benefits relative to the baseline, reflecting enhanced pulp dispersion and cleaner chalcopyrite surfaces. As shown Figure 14, the highest recovery, 47.6 percent at 2.97 percent Cu grade, was obtained with 150 g/t FreeFlote-2244, indicating a strong response of the montmorillonite-dominated ore to polymeric dispersant treatment. The observed behavior is consistent with electrokinetic results showing a marked increase in negative surface potential, which promotes the separation of clay fines from mineral surfaces and stabilizes hydrodynamic conditions during flotation.

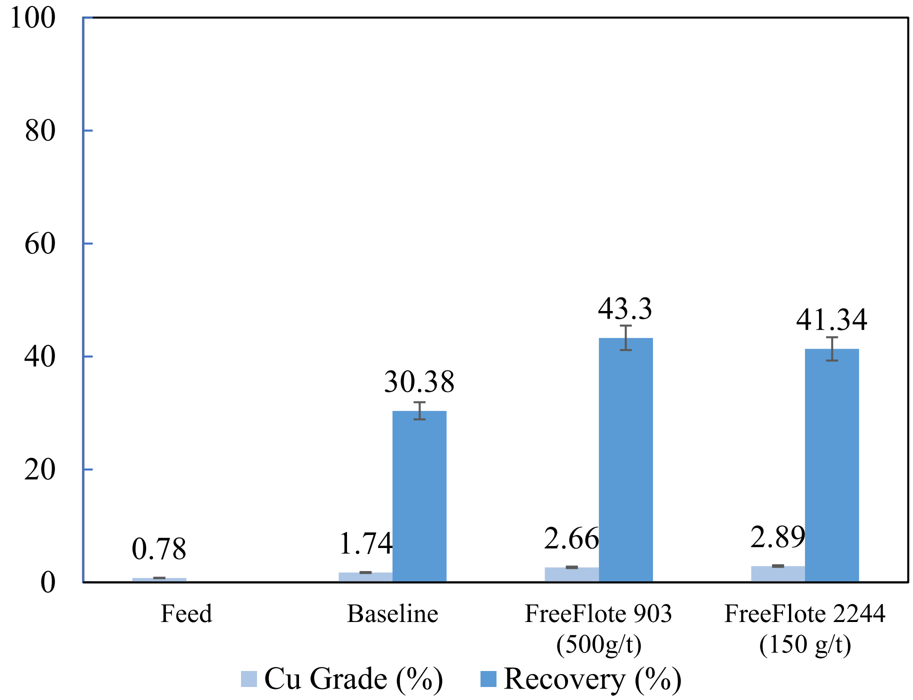

Figure 15. Comparative performance of FreeFlote-903 and FreeFlote-2244 on the North America copper ore.

At equivalent operating conditions, FreeFlote-2244 (150 g/t) demonstrates superior recovery and grade performance compared to FreeFlote-903 (500 g/t), with values of 47.6 percent and 2.97 percent Cu, respectively. The stronger efficiency of FreeFlote-2244 is attributed to its higher anionicity and molecular flexibility, which better target the electropositive sites on swelling clays, effectively reducing pulp viscosity and preventing slime coatings. The results confirm that dispersant efficiency in swelling clay–rich systems depends primarily on charge density and molecular interaction rather than on dosage alone.

4 Conclusions

Collectively, the electrokinetic data demonstrates that the response of flotation systems to dispersants and pH regulators depends on a delicate interplay between mineral surface chemistry, reagent functionality, and clay structure. The non-swelling clays (kaolinite and muscovite) respond strongly to anionic polymer dispersants, showing enhanced negative surface charge and improved dispersion. In contrast, swelling clays (montmorillonite) exhibit limited zeta potential modification due to their permanent layer charge and high hydration energy, implying that polymer adsorption is sterically and electrostatically constrained.

Moreover, the choice of pH regulator critically affects the efficiency of these reagents. Sodium hydroxide maintains strong negative potentials conducive to clay dispersion, whereas calcium-bearing alkalinity induces charge reversal and surface bridging—advantageous for pyrite depression but unfavorable for maintaining pulp fluidity. Hence, the optimal combination of dispersant chemistry and pH regulation must balance selectivity and stability within high-clay flotation circuits.

These findings reinforce the concept that controlling clay behavior in flotation requires not only reagent optimization but also a mechanistic understanding of surface charge evolution under realistic pulp conditions. By integrating zeta potential measurements with rheological and flotation performance data, this work establishes a framework for designing tailored reagent strategies that enhance recovery and selectivity in complex, clay-rich ore systems.

Rheological characterization revealed that the untreated copper ore containing 15 wt% montmorillonite displayed pronounced shear-thinning and thixotropic behavior, characterized by high apparent viscosity at low shear rates and gradual structural rebuilding over time. This indicates the presence of a flocculated network typical of swelling clays, where interparticle associations dominate the suspension structure. In practical flotation systems, where local shear rates are relatively low and vary spatially, such non-Newtonian behavior leads to poor slurry mobility, hindered bubble–particle interactions, and uneven solids distribution. The observed decrease in viscosity with increasing shear rate confirms that the clay network can only be broken down under intense mechanical stress, a condition that cannot be uniformly achieved within flotation cells.

The addition of dispersant reagents fundamentally improved this behavior. Both FreeFlote-903 and FreeFlote-2244 reduced apparent viscosity and yield stress, suppressing the thixotropic rebuilding tendency and transforming the slurry response toward near-Newtonian flow. FreeFlote-2244 produced a slightly greater viscosity reduction and more stable rheological profile across the entire shear-rate range, indicating more efficient dispersion of montmorillonite platelets. This stabilization is critical in flotation circuits, where shear conditions within cells are limited compared to pumps or pipelines. Maintaining a stable, low-viscosity, and near-Newtonian suspension ensures uniform mixing, better gas dispersion, and consistent hydrodynamics, ultimately enabling improved flotation performance under realistic plant conditions.

The flotation test results clearly highlight that dispersant chemistry exerts a decisive influence on metallurgical performance in high-clay copper ores. For the Latin America ore, characterized by non-swelling phyllosilicates such as muscovite and chlorite, both FreeFlote-903 and FreeFlote-2244 improved recovery relative to the baseline, with FreeFlote-2244 providing the highest Cu recovery (75.1%) at comparable grade (4.9%). The enhanced flotation response is attributed primarily to improved surface cleaning and inhibition of slime coating rather than bulk rheology modification, consistent with the electrokinetic evidence showing increased surface charge separation between chalcopyrite and clays.

In contrast, the NA ore, dominated by montmorillonite, exhibited stronger dispersant dependence, with flotation recovery increasing proportionally with polymer dosage. FreeFlote-2244 outperformed FreeFlote-903 at all dosages, achieving up to 47.6% Cu recovery at 2.97% grade, confirming its superior interaction with swelling clays through enhanced electrostatic repulsion and viscosity reduction. The comparative results demonstrate that while both reagents effectively mitigate clay-related losses, the optimal dispersant strategy depends on the dominant clay type: moderate dosing for non-swelling systems and higher anionic polymer concentrations for swelling systems.

To sum up, these findings underscore that tailoring dispersant structure and dosage to ore-specific clay mineralogy provides a powerful means of improving flotation efficiency, enhancing concentrate quality, and stabilizing circuit performance in complex, high-clay copper operations.

By embracing interdisciplinary collaboration—spanning mineralogy, surface chemistry, rheology, process engineering, and data science—we can transform the clay challenge from a persistent liability into a manageable, even predictable, aspect of modern mineral processing.

The path forward requires that Nalco Water continue to invest in fundamental research while maintaining close partnerships with industry to ensure that laboratory discoveries translate into robust, scalable solutions.

As this study will demonstrate, the tools, knowledge, and collaborative spirit needed to advance clay management are within our grasp. The question is not whether we can overcome the clay challenge, but how quickly we can deploy these innovations to secure the sustainable supply of base metals essential for the global energy transition and technological advancement.

References

[1] Batista e Silva, G. V., Oliveira, G. J. R., & Horta, D. G. (2024). On the Use of Styrene-Based Nanoparticles to Mitigate the Effect of Montmorillonite in Copper Sulfide Recovery by Flotation. *Polymers*, 16(12), 1682. https://doi.org/10.3390/polym16121682

[2] Li, Z., Li, Z., Rao, F., et al. (2018). Slime coating of kaolinite on chalcopyrite in saline water flotation. *International Journal of Minerals, Metallurgy and Materials*, 25(5), 494-503. https://doi.org/10.1007/S12613-018-1594-7

[3] Leiva, W. H., Toro, N., Robles, P., et al. (2025). Rheology Modifying Reagents for Clay-Rich Mineral Suspensions: A Review. *Polymers*, 17(17), 2427. https://doi.org/10.3390/polym17172427

[4] Luo, K., Sun, C., & Sun, T. (2024). Variability of lead-zinc sulfide ore slurry rheological properties and its influence on flotation conditions. *Physicochemical Problems of Mineral Processing*, 60(4), 192663. https://doi.org/10.37190/ppmp/192663

[5] Ramirez-Madrid, A., Irribarra, K., Gutierrez, L., et al. (2024). Effect of sodium silicate modified with Fe^{2+} and Al^{3+} as dispersant on flotation of molybdenite and chalcopyrite in

presence of kaolinite and seawater. *Minerals Engineering*, 208, 108551. https://doi.org/10.1016/j.mineng.2023.108551

[6] Li, C., Wu, Z., Wu, Z., et al. (2024). Effect of the Interaction between Clays and Cations on Froth Rheology in Flotation. *Minerals*, 14(7), 706. https://doi.org/10.3390/min14070706

[7] Yepsen, R., Roa, J., Toledo, P. G., et al. (2021). Chalcopyrite and Molybdenite Flotation in Seawater: The Use of Inorganic Dispersants to Reduce the Depressing Effects of Micas. *Minerals*, 11(5), 539. https://doi.org/10.3390/MIN11050539

[8] Molaei, N., Forster, J., Shoaib, M., et al. (2022). Efficacy of sustainable polymers to mitigate the negative effects of anisotropic clay minerals in flotation and dewatering operations. *Cleaner Engineering and Technology*, 8, 100470. https://doi.org/10.1016/j.clet.2022.100470

[9] Liu, D., & Peng, Y. (2014). Exploring the different dispersion effect of anionic polymeric dispersant on clay minerals in the flotation using fresh and saline water. *Proceedings of the 27th International Mineral Processing Congress*.

[10] Rulyov, N. N. (2025). Separation of Ultrafine Bentonite Suspension by Ultraflocculation and Sedimentation-Microflotation in Inclined Tubular Separator. *Journal of Mining and Metallurgical Sciences*, 11(21). https://doi.org/10.54026/jmms/1121

[11] Wani, O. B., Manzoor, S., Molaei, N., et al. (2022). Beneficiation of Nickel from Ultramafic Ores: Using Sodium Citrate as a Green Processing Reagent. *Resources, Conservation and Recycling*, 186, 106496. https://doi.org/10.1016/j.resconrec.2022.106496

[12] Galleguillos Madrid, F. M., Arancibia-Bravo, M. P., Sepúlveda, F. D., et al. (2023). Ultrafine Kaolinite Removal in Recycled Water from the Overflow of Thickener Using Electroflotation: A Novel Application of Saline Water Splitting in Mineral Processing. *Molecules*, 28(9), 3954. https://doi.org/10.3390/molecules28093954

[13] Soliz, Á., Galleguillos Madrid, F. M., Cobos-Murcia, J. A., et al. (2024). Electrochemical Performance of Ti Gr. 2 as Electrodes in Contact with Saline Suspension of Clays during the Electroflotation Process. *Applied Sciences*, 14(19), 8825. https://doi.org/10.3390/app14198825

[14] Chimonyo, W., Chen, J., & Peng, Y. (2024). Synergistic effects of Reflux Flotation Cell's downcomer and reverse fluidization bed in rejecting clay entrainment during particle separation. *Powder Technology*, 440, 119796. https://doi.org/10.1016/j.powtec.2024.119796

[15] Chen, X., & Peng, Y. (2018). Managing clay minerals in froth flotation—A critical review. *Mineral Processing and Extractive Metallurgy Review*, 39(5), 289 307. https://doi.org/10.1080/08827508.2018.1433175

[16] Wang, Y. (2016). Mitigating the deleterious effect of clay minerals on copper flotation. PhD Thesis, University of Queensland. https://doi.org/10.14264/UQL.2017.49